



IN SILICO EXAMINATION OF ANTIMICROBIAL ACTIVITY OF BENZOXAZOLE DERIVATIVES AGAINST DIHYDROFOLATE REDUCTASE

Kritika Maheshwari^{1*}, Dr. Nasiruddin Ahmad Farooqui², Mr. Mohd Salman³, Mrs. Preeti Yadav⁴

¹. Research scholar, Translam Institute of Pharmaceutical Education and Research Meerut, India

². Guide, Translam Institute of Pharmaceutical Education and Research Meerut, India

³. Assistant Professor, Translam Institute of Pharmaceutical Education and Research Meerut, India

⁴. Drug Regulatory Affairs Executive, Synmedic Laboratories, Gurugram, India

*Corresponding author

Email id – kritikamaheshwari1110@gmail.com

ABSTRACT :

Antimicrobial resistance has become one of the most crucial threat to public health due to the ability of microbes resistance against antimicrobial drugs. The escalating threat posed by antimicrobial resistance underscores the urgent necessity for the development of targeted therapeutic strategies and enhanced international collaboration to effectively mitigate the global impact of AMR. To oppose drug resistance we introduce more potent drug by using in silico approaches with the help of drug designing methods. We built the model against a Gram-positive bacterial strain using the co-crystallized ligand from the Dihydrofolate Reductase protein (PDB ID: 6PR7). Ligand-based study was performed on 63 benzoxazole derivatives. With help of molecular docking studies shows that PF7 emerges as the best docked compound with docking score (-4.368 kcal/mol). A four-point pharmacophore model was created using the dataset, and based on this model, an atom-based 3D-QSAR model was developed. The model showed good statistical values, with a correlation coefficient of $Q^2 = 0.7380$ for the training set and $R^2 = 0.9793$ for the test set, proving its reliability. The best-docked compound was selected and used to perform ligand-based virtual screening through the PubChem database. After that, to ensure their safety and effectiveness. ADMET (absorption, distribution, metabolism, excretion, and toxicity) studies were done on the top 10 screened compounds. Overall, the results suggest that these compounds could be promising inhibitors of Dihydrofolate Reductase and may be useful in treating microbial infections.

Keywords: In silico ; antimicrobial; molecular docking; 3D-QSAR; ADMET; pharmacophore hypothesis.

1.0 Introduction

The growing threat of antimicrobial resistance (AMR) has become a critical global health concern, undermining the efficacy of existing antibiotics and leading to increased rates of treatment failure, prolonged illness, and mortality (1, 2). Among the various resistant pathogens, *Staphylococcus aureus*, particularly methicillin-resistant *Staphylococcus aureus* (MRSA), has emerged as a major cause of infections in both healthcare and community settings (3). The resistance of *S. aureus* to conventional antibiotics such as trimethoprim and β -lactams has made the treatment of common bacterial infections increasingly difficult (4). This highlights an urgent need for novel therapeutic agents that can effectively target resistant strains. One promising approach involves focusing on essential bacterial enzymes, such as dihydrofolate reductase (DHFR), (5) which plays a crucial role in folate metabolism and is necessary for DNA synthesis and cell proliferation. Despite being a well-established target, there is a continuing need for selective and potent DHFR inhibitors that can overcome existing resistance mechanisms.

This research aims to explore the antimicrobial potential of benzoxazole derivatives as inhibitors of *Staphylococcus aureus* DHFR through in silico approaches. The study is designed to identify structurally active benzoxazole compounds (6, 7, 8) develop a pharmacophore hypothesis (9) that captures the key features required for DHFR inhibition, build and validate a 3D-QSAR model to predict biological activity (10), and perform molecular docking to analyze interactions between the compounds and the DHFR binding site, particularly using structural insights from PDB ID: 6PR7 (11). Additionally, virtual screening will be employed to identify new lead molecules, and ADMET profiling will be conducted to evaluate their drug-likeness and safety.

The significance of this study lies in its potential to contribute to the discovery of new antimicrobial agents capable of addressing drug resistance in *S. aureus*. Utilizing benzoxazole as a pharmacophoric scaffold leverages its known pharmacological versatility, while the integration of computational methods offers a cost-effective and time-efficient strategy for drug development. By identifying promising DHFR inhibitors, this research supports the global effort to mitigate the impact of AMR and provides a foundation for future experimental validation and therapeutic advancement (12).

2.0 Material and method

This chapter provides a thorough explanation of the software and publicly available web resources utilized for analysis. Details on the techniques employed for the theoretical and experimental studies are provided.

2.1 Application software and web-based software

Schrodinger's suite (Maestro version 13.6), LLC, New York, 2022, is used for computational investigations such as molecular docking, pharmacophore hypothesis creation, QikProp experiments, 3D-QSAR model generation, and virtual screening. Online research was done for non-profit, publicly available web tools such as PubChem and ProTox-II.

2.2 Methods

2.2.1 Ligand-based drug design

2.2.1.1 Dataset

Molecular docking was conducted on the dataset of all 63 benzoxazole derivatives that had been synthesized before and had varying MIC₅₀ against *Staphylococcus aureus* species. The dataset was retrieved and collated from the published work (Table 2.2.1). Additionally, the MIC₅₀ value was transformed into pMIC₅₀ [-log₁₀ (MIC₅₀)] for the purpose of developing pharmacophore hypotheses and the 3D-QSAR model (13).

2.2.1.2 The generation of 3D X-ray crystallographic structure of *S. aureus* dihydrofolate reductase co-crystallized with benzyl-dihydrophthalazine inhibitor and NADP(H) (6PR7)

The protein dihydrofolate reductase 3D structure of the mutation-free (PDB ID: 6PR7, resolution 2.01 Å) was obtained from the Protein Data Bank (PDB) (<https://www.rcsb.org/structure/6PR7>) (14). In the 6PR7 structure, the protein is derived from *Staphylococcus aureus* (strain NCTC 8325) and crystallized at 2.01 Å resolution, providing high-resolution insight into the binding interactions of DHFR with the antifolate drug Methotrexate and the cofactor NADPH. The structure was determined by X-ray diffraction. To see the dihedral angles ψ against ϕ of the amino acid residues in the protein structure, the Ramachandran plot was employed. It shows the empirical distribution of the data points in a single structure. The red and yellow spots on the plan represented the places that were extensively vetted and showed potential.

2.2.1.3 Protein preparation and a grid generation for selected target Dihydrofolate reductase

After obtaining the PDB ID using the protein production wizard, the protein was examined for extraneous atoms and chains, unbound ligands, and water molecules. Grid creation was made possible by the Glide module following the inclusion of hydrogen bonds and missing residues. A protein's structure was refined and its energy was minimized using the OPLS-2005 force field. (15)

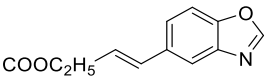
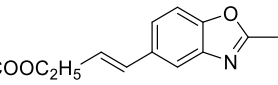
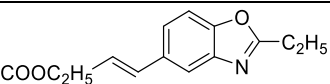
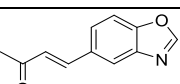
2.2.1.4 Preparation of ligands

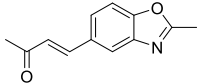
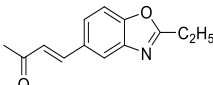
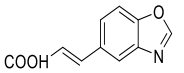
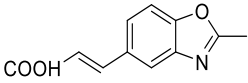
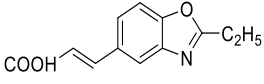
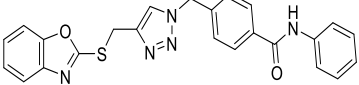
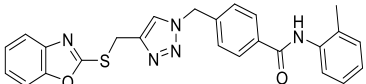
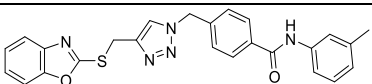
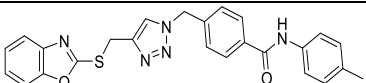
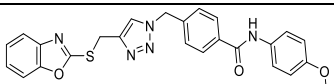
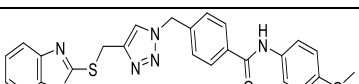
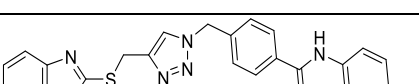
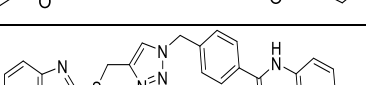
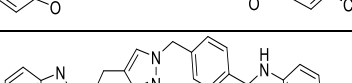
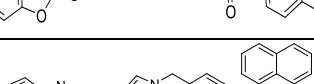
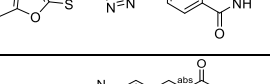
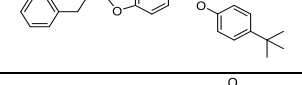
Using ChemDraw 16.0, all 63 of the gathered benzoxazole derivatives were sketched in two dimensions. The LigPrep module (2022, Schrodinger, LLC, NY) was then used to convert them into three dimensions (16). Each ligand was created by choosing it from the LigPrep module's Project table. No conformers were produced for the compounds, and they were neutralized with ionization states adjusted at a pH 7.4±0.0 with a maximum ligand size of 500 atoms. The energy minimization was done using the OPLS-2005 force field.

2.2.1.5 Molecular docking

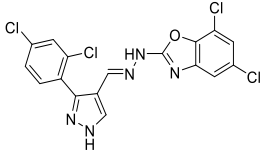
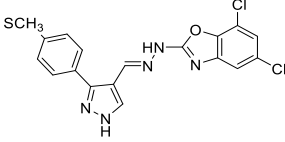
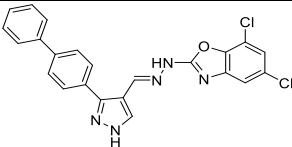
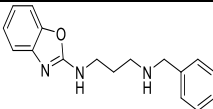
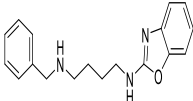
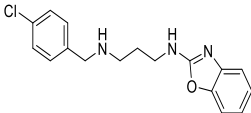
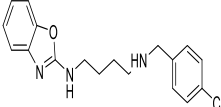
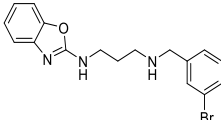
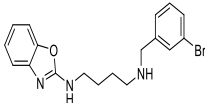
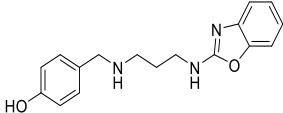
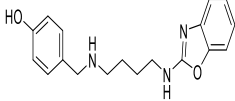
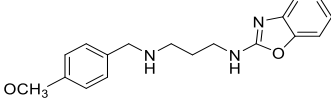
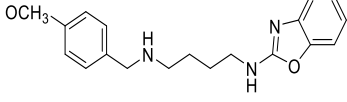
The preferred orientation for ligand-receptor binding is predicted via molecular docking. The active pocket site of the protein dihydrofolate reductase (PDB ID: 6PR7) was docked with all 63 of the generated ligands using a Glide module. For the optimal orientation of the ligand and protein, the "Extra precision mode" from the ligand docking of a gliding module was employed. The program's ligand interaction tool was used to verify the best docked compound's 2D and 3D ligand-protein interaction after it was selected based on docking scores (17).

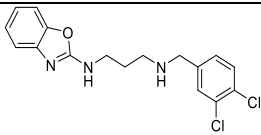
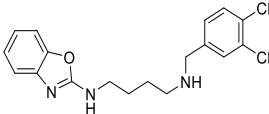
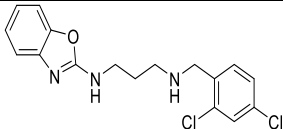
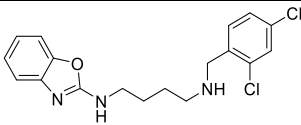
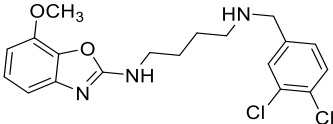
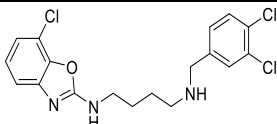
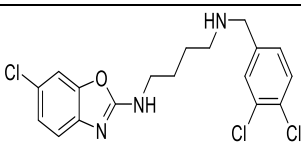
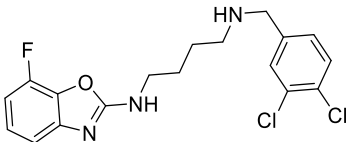
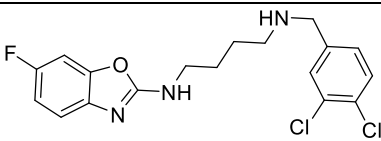
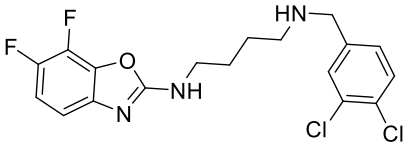
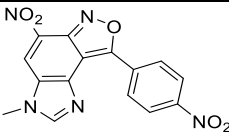
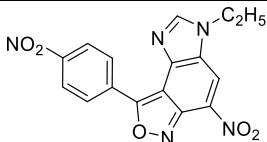
Table 2.2.1: Library of benzoxazole derivatives with MIC values (μg/ml)

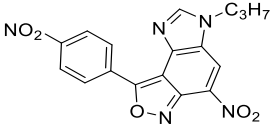
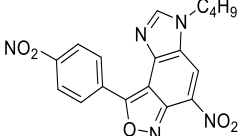
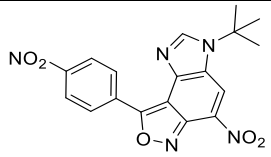
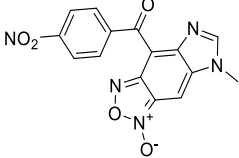
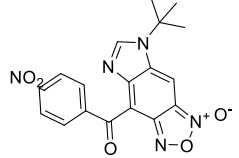
S. No.	Compounds	Chemical Structures	MIC ₅₀ (μg/ml)
1	PA1		1.558749
2	PA2		1.460992
3	PA3		1.243534
4	PA4		1.230913

5	PA5		1.701633
6	PA6		1.429853
7	PA7		0.954633
8	PA8		1.052651
9	PA9		1.081627
10	PB1		3.591862
11	PB2		3.318082
12	PB3		3.926133
13	PB4		3.926133
14	PB5		3.347183
15	PB6		3.979522
16	PB7		3.628862
17	PB8		3.355342
18	PB9		4.336134
19	PB10		3.682985
20	PC1		2.453808
21	PC2		3.095232

22	PC3		2.471075
23	PC4		0.727224
24	PC5		1.042623
25	PC6		0.33694
26	PC7		2.792356
27	PC8		2.526397
28	PC9		2.419161
29	PC10		2.748963
30	PC11		0.654706
31	PD1		1.554688
32	PD2		1.83305
33	PD3		1.561607

34	PD4		1.547617
35	PD5		1.825608
36	PD6		1.554668
37	PE1		0.643067
38	PE2		0.664201
39	PE3		1.596322
40	PE4		1.31417
41	PE5		1.653526
42	PE6		1.369077
43	PE7		0.968118
44	PE8		0.988141
45	PE9		0.687111
46	PE10		1.007268

47	PE11		1.340246
48	PE12		1.357303
49	PE13		1.641276
50	PE14		1.658333
51	PE15		1.692737
52	PE16		2.299627
53	PE17		2.299627
54	PE18		2.582359
55	PE19		2.582359
56	PE20		2.602331
57	PF1		0.433623
58	PF2		0.570408

59	PF3		0.661955
60	PF4		0.84095
61	PF5		0.706251
62	PF6		1.831307
63	PF7		2.103929

2.2.1.6 A Pharmacophore model generation

The potential interactions between ligand-receptor complexes are identified and extracted using a ligand-based pharmacophore model, which is an ensemble of similar steric and electronic properties. The pharmacophore model was made using a PHASE module. A PHASE module is a multicomputed product used for 3D-QSAR model creation, pharmacophore modeling, and structural alignment.

Initially, all 63 designed ligands were aligned using the ligand alignment tool in the PHASE module. After aligning them, different molecular shapes (conformers) were generated for each ligand—up to 50 per structure. The compounds were then categorized based on their antimicrobial activity: those with a pMIC50 value of 0.65 or higher were labeled as *active*, while those with lower values were considered *inactive*. To build a pharmacophore model—a kind of chemical pattern that describes the features necessary for biological activity—six key features were considered: hydrophobic regions (H), hydrogen bond donors (D), hydrogen bond acceptors (A), positively charged groups (P), negatively charged groups (N), and aromatic rings (R). Out of the 63 ligands, 42 were found to be active, 3 inactive, and the rest showed moderate activity.

Using this information, four unique pharmacophore hypotheses were generated, with each model containing up to five key features (18). The best-performing hypothesis was chosen based on its ability to correctly identify active and inactive compounds. The top model, named *AARR_1*, consisted of four key pharmacophoric features and is detailed in Table 2.2.2.

To test the reliability of this hypothesis, it was validated using a set of 109 *decoy* compounds (inactive compounds with similar properties) taken from the DUD-E database, along with the 42 active ligands. The total dataset of 151 compounds was used to evaluate the model's accuracy using various statistical methods: Enrichment Factor (EF at 1%), BEDROC (a measure of early recognition), RIE (initial ranking quality), ROC (overall model performance), and AUAC (how well the model ranks actives higher than inactives). All these scores range from 0 to 1, where 1 is ideal (19).

Finally, A 3D-QSAR model was constructed using this validated pharmacophore model in order to gain a better understanding of the structural characteristics that give rise to antimicrobial action.

Table 2.2.2: All 4 generated hypothesis by PHASE module and their parametric scores.

Hypothesis	Survival Score	Site Score	Vector Score	Volume Score
AARR_2	5.223	0.721	0.922	0.594
AARR_1	5.244	0.725	0.925	0.598
AARR_3	5.204	0.708	0.892	0.604

AARR_4 5.201 0.700 0.905 0.501

2.2.1.7 Atom based 3D-QSAR model

The 3D-QSAR approach aims to establish a statistical correlation between the three-dimensional structural properties of ligands and their biological activity using mathematical modeling techniques. In this study, an atom-based 3D-QSAR model was constructed using the PHASE module integrated within Schrodinger's Maestro software (version 13.6) (20).

For the development of the QSAR model, the most reliable pharmacophore hypothesis, *AARR_1*, was selected, encompassing a total of 67 ligands. These compounds were randomly divided into two sets: a *training set* comprising 67.2% of the ligands (39 compounds) and a *test set* with the remaining 32.7% (19 compounds), as presented in Table 2.2.3 (21).

The atom-based QSAR modeling employed a maximum of four Partial Least Squares (PLS) factors with a grid spacing of 1 Å. To evaluate the internal predictive accuracy of the model, a Leave-One-Out (LOO) cross-validation method was applied. The model included six distinct molecular features: negatively charged groups (N), positively charged groups (P), hydrogen bond donors (D), hydrophobic regions (H), electron-withdrawing groups (W), and miscellaneous features (X) (22).

To facilitate the understanding of how molecular structures influence activity, a QSAR visualization was performed using both the most active and the least active compounds in the dataset, thereby supporting structural optimization and future ligand design.

Table 2.2.3: Dataset of Atom based 3D-QSAR model built by AARR_1 hypothesis with their docking score, observed and predicted activity (pMIC₅₀).

Compound no.	QSAR set	Observed activity	Predicted activity	Docking score
PA1	Training	1.558	0.984	-5.584
PA2	Test	1.460	2.158	-5.566
PA3	Training	1.243	2.520	-5.774
PA4	Training	1.230	2.543	-5.514
PA5	Training	1.701	2.346	-5.342
PA6	Training	1.429	1.692	-5.808
PA7	Test	0.954	2.499	-5.342
PA8	Test	1.052	2.093	-5.571
PA9	Test	1.081	1.428	-5.572
PB1	Test	3.591	3.545	-6.038
PB2	Test	3.318	3.547	-7.511
PB3	Training	3.926	4.070	-5.693
PB4	Training	3.926	3.607	-3.361
PB5	Training	3.347	3.400	-5.016
PB6	Test	3.979	1.617	-5.016
PB7	Training	3.628	3.56756	-4.876
PB8	Training	3.355	3.585	-3.854
PB9	Test	4.336	3.590	-4.624
PB10	Test	3.682	2.930	-6.366
PC1	Training	2.453	2.392	-6.436
PC2	Training	3.095	3.108	-7.575
PC3	Training	2.471	1.079	-5.42
PC4	Training	0.727	2.441	-6.235
PC5	Training	1.042	0.970	-5.833
PC6	Training	0.336	0.427	-2.751
PC7	Training	2.792	2.833	-8.572
PC8	Training	2.526	2.461	-6.612
PC9	Test	2.419	0.894	-3.546

PC10	Test	2.748	1.474	-5.745
PC11	Test	0.654	1.758	-6.396
PD1	Training	1.554	1.490	-6.466
PD2	Training	1.833	1.010	-7.314
PD3	Training	1.561	1.624	-7.126
PD4	Test	1.547	1.809	-4.877
PD5	Test	1.825	1.768	-5.969
PD6	Test	1.554	1.952	-8.51
PE1	Test	0.643	1.142	-6.558
PE2	Training	0.664	0.836	-5.638
PE3	Training	1.596	1.154	-5.85
PE4	Training	1.314	1.359	-4.596
PE5	Test	1.653	1.694	-5.587
PE6	Training	1.369	1.447	-4.744
PE7	Training	0.968	0.929	-3.8
PE8	Training	0.988	0.972	-5.355
PE9	Training	0.687	0.872	-4.479
PE10	Training	1.007	1.063	-5.672
PE11	Training	1.340	0.960	-5.006
PE12	Training	1.357	2.243	-4.788
PE13	Training	1.641	1.617	-5.27
PE14	Training	1.658	1.681	-5.023
PE15	Training	1.692	1.830	-4.546
PE16	Training	2.299	2.270	-4.708
PE17	Training	2.299	2.315	-4.541
PE18	Test	2.582	2.275	5.819
PE19	Training	2.582	2.321	-4.783
PE20	Test	2.602	2.540	-4.953
PF1	Training	0.433	0.596	-3.441
PF2	Training	0.570	0.645	-2.744
PF3	-	0.661	-	-4.839
PF4	-	0.840	-	-4.774
PF5	-	0.706	-	-3.341
PF6	-	1.831	-	5.051
PF7	-	2.103	-	-4.771

2.2.1.8 Molecular docking based virtual screening

Virtual screening is a computational technique employed in drug discovery to explore huge chemical libraries and identify small molecules that are probably to bind effectively to a specific biological target. In this study, the PubChem database—a freely accessible repository of chemical structures and bioactivity data—was utilized to identify potential lead compounds. The most promising docked compound, designated as PC7, was used as a reference to perform a structural similarity search within PubChem. This search yielded a total of 67 structurally similar compounds (hit leads). The 2D structures of these hit molecules were subsequently downloaded and subjected to molecular docking studies against the target protein, dihydrofolate reductase. Docking was performed using the Extra Precision (XP) mode to ensure accurate prediction of ligand–protein binding orientations. From these, the top 10 compounds showing the highest binding affinity and favorable interaction profiles were selected for further pharmacokinetic (ADME) and toxicity evaluations (22).

2.2.1.9 *In silico* ADME screening and toxicity predictions

Pharmacokinetics characteristics, including absorption, distribution, metabolism, excretion, and toxicity profiles of the compounds, were assessed using the QikProp module (2022, Schrodinger, LLC, NY) and the ProTox-II web tool in order to enhance the safety, quality, and effectiveness of a medication (23). Intestinal absorption, blood-brain barrier permeability, CYP inhibition, and total clearance rate are some of the variables that affect the ADME profile. Hepatotoxicity, mutagenicity, carcinogenicity, and immunotoxicity can all be assessed using toxicity profiles, both subjectively and quantitatively (24). Additionally, the top ten virtually screened compounds underwent ADME and toxicity profile analyses, which provide valuable information about the pharmaceuticals' ADME in the body along with their toxicity effects (25).

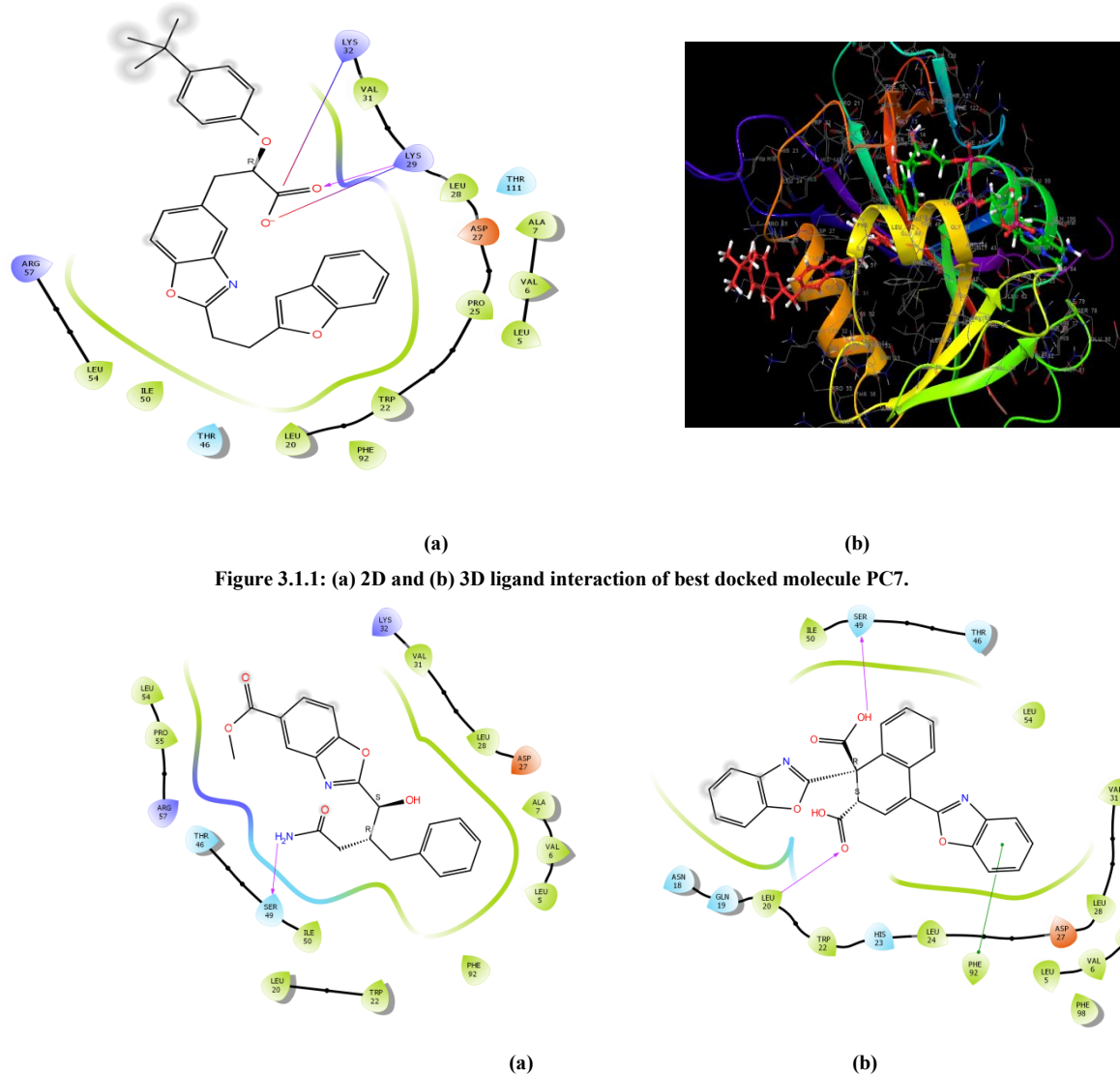
3.0 Results and Discussion

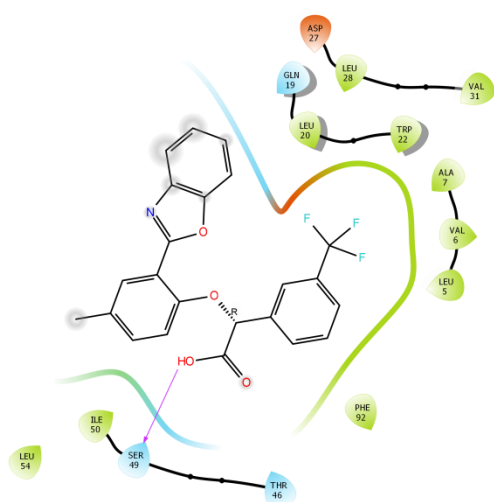
3.1 Ligand-based drug design

3.1.1 Molecular docking

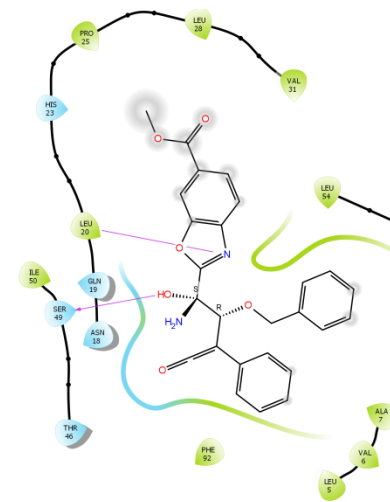
The docking was performed for 63 benzoxazole derivatives and compared with the standard drugs used – ciprofloxacin, ceftriaxone and cefotaxime. From the results shown, it was cleared that PC7 compound showed the best docking score (-8.572 kcal/mol) and discovered to be more active as compared to the standard drugs ceftriaxone (-7.039 kcal/mol), cefotaxime (-5.778 kcal/mol) and Ceftriaxone (-7.039 kcal/mol). It showed that compound PC7 found to be had One hydrogen bonding with the amino acid residue (C=O....LYS29) and two salt bridge (O⁻ ...LYS29 , O⁻ ...LYS32) (Figure 4.1.1) (Table3.2.3).

Further, the best docked active compound was screened for drug similarity from the PubChem database and the obtained 67 compounds were then put through for XP docking with the protein dihydrofolate reductase. The obtained result showed that, compound CID 174377141 had the best docking score (-9.934 kcal/mol) against the standard drugs ceftriaxone (-7.039 kcal/mol), Ciprfloxacin (-7.254 kcal/mol) and cefotaxime (-5.778 kcal/mol). The compound CID 174377141 had one H-bond with amino acid residue (NH₂...SER49), considered being the most active and has higher binding affinity among all the hits compound thus outspacing the standard drugs. The top 10 hit lead ligand-amino acid residues were shown in Table 3.1.1).

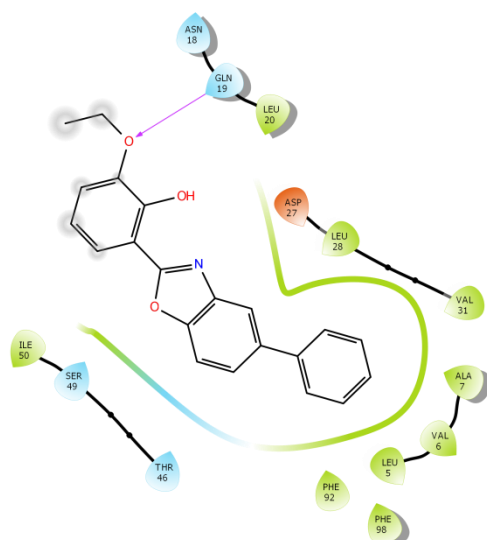




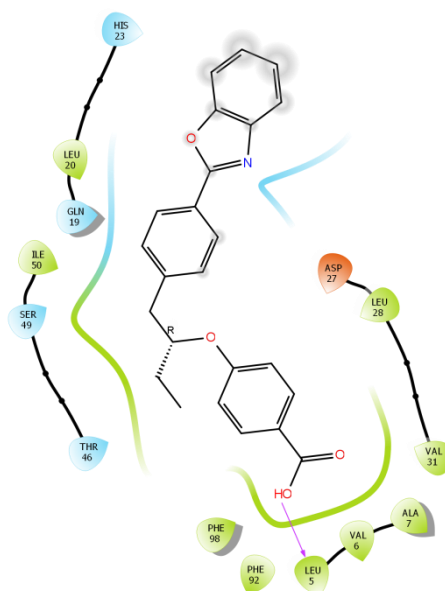
(c)



(d)



(e)



(f)

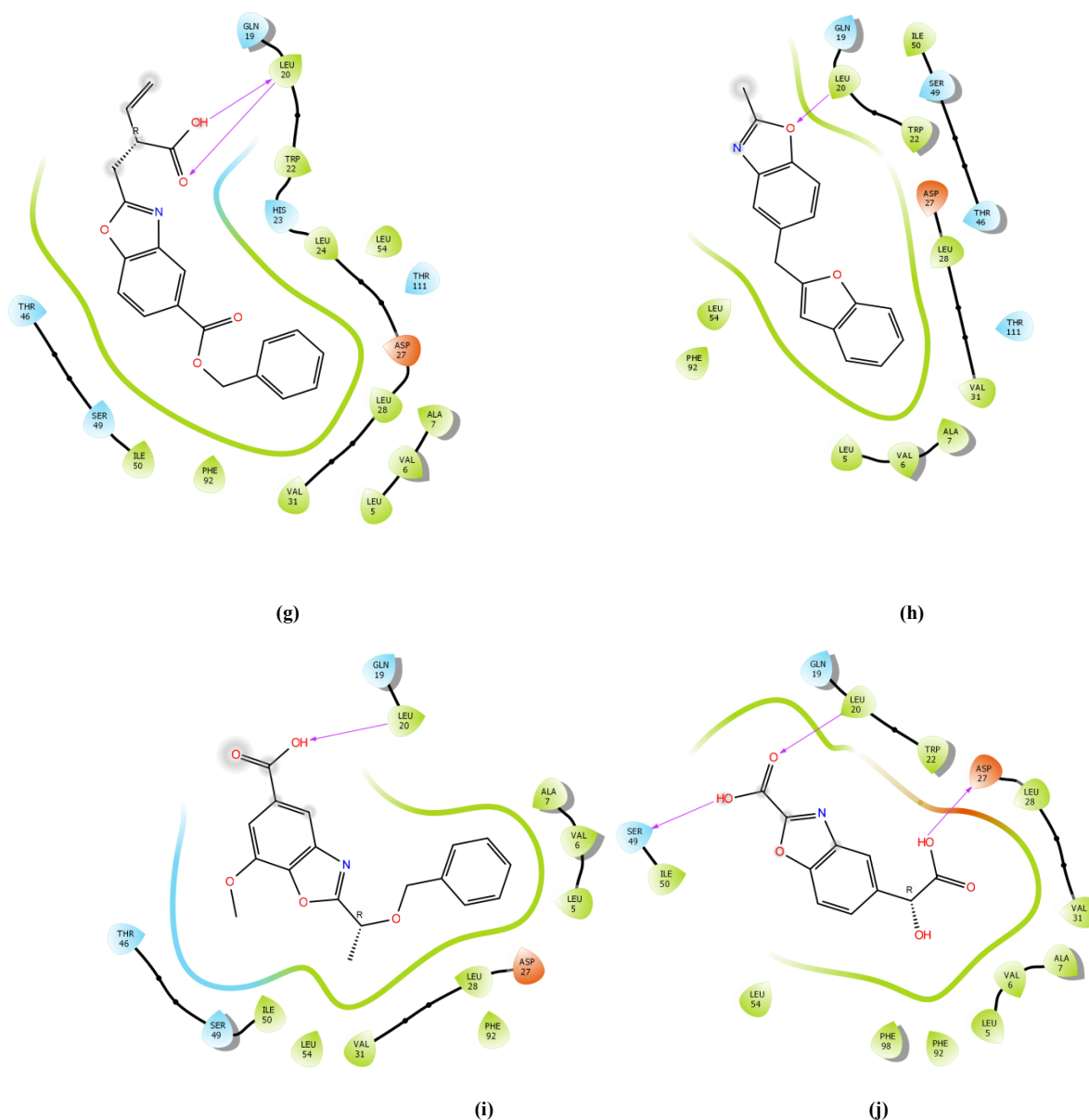
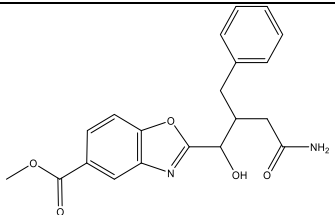
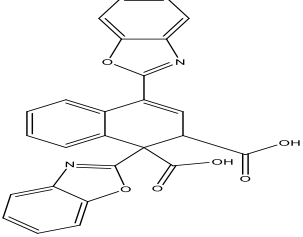
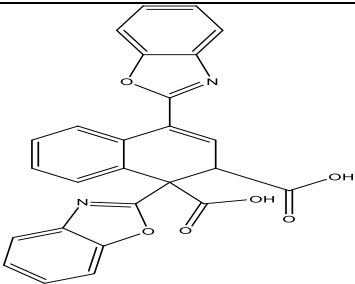
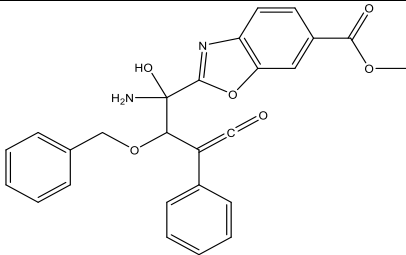
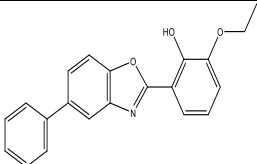
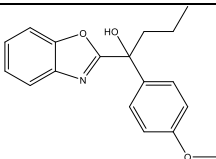
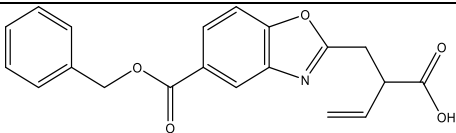
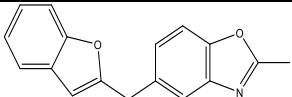
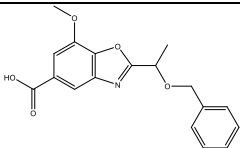
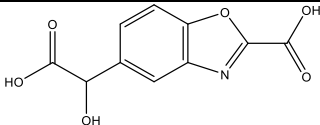
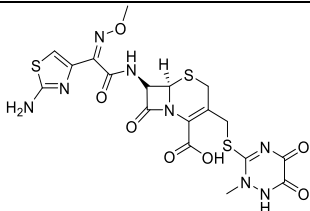


Figure 3.1.2: 2D ligand interaction and surface binding of derivative (a) CID 174377141 (b) CID 172743839 (c) CID 162579096 (d) CID 174331251 (e) CID 163955800 (f) CID 175567519 (g) CID 166872478 (h) CID 163583501 (i) CID 165521246 (j) CID 165349091

S.NO	Compounds	Chemical structure	Docking score
1	174377141		-9.934
2	172743839		-9.910

3	162579096		-9.714
4	174331251		-9.647
5	163955800		-9.392
6	175567519		-8.527
7	166872478		-8.493
8	163583501		-8.490
9	165521246		-8.357
10	165349091		-8.307
11	Ceftriaxone		-7.039

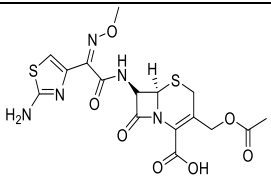
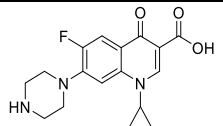
12	Cefotaxime		-5.778
13	Cirprofloxacin		-7.254

Table 3.1.1: XP docking results of the 10 topmost compounds against the protein dihydrofolate reductase (PDB ID: 6PR7).

Table 3.1.2: Ligand-Amino acid residues interactions of the 10 topmost docked compounds.

S. no.	Ligand	H-bond interactions	Other interactions
1	174377141	SER 49	-
2	172743839	LEU 20, SER 49	Pi-Pi stacking: PHE 92
3	162579096	SER 49	-
4	174331251	LEU 20, SER 49	-
5	163955800	GLN 19	-
6	175567519	LEU 5	-
7	166872478	LEU 20	-
8	163583501	LEU 20	-
9	165521246	LEU 20	-
10	165349091	LEU 20, SER 49, ASP 27	-

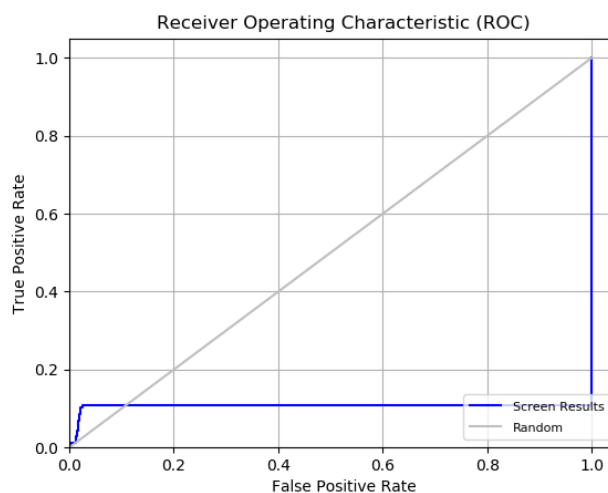
3.1.2 Pharmacophore hypothesis analysis

The 4-point hypothesis AARR_1 was chosen as the best of the 4 generated hypotheses based on their volume score (0.598), vector score (0.925), site score (0.725), and survival score (5.244) (Table 2.2.2). The decoy dataset (DUD-e database), which contains 151 compounds (109 decoys and 42 actives), was then used to validate the best chosen hypothesis.

The verified AARR_1 hypothesis had a ROC (receiver operating characteristics) of 0.11, an Enrichment factor (1%) of 1.30, a Phase hypo score of 1.11, an AUAC (area under accumulation curve) of 0.54, a robust initial enhancement (RIE) of 1.58, and a BEDROC160.9 of 0.04. Sensitivity (true positive rate) on the X-axis and specificity (false positive rate) on the Y-axis were plotted in a ROC analysis. Active compounds are ranked higher than inactive ones if the curve exhibits a sharp rise towards the upper left corner and flattens out with a value nearer 1.

The accuracy of the developed pharmacophore model AARR_1 is demonstrated graphically by the curve that begins in the upper left corner and flattens at the end, with a ROC value of 0.11 (Figure 3.1.3). According to the best theory, an activity requires two hydrogen bond acceptors, and two aromatic ring characteristic (Figure 3.1.4).

Figure 3.1.3: A ROC plot of the best generated hypothesis AARR 1.



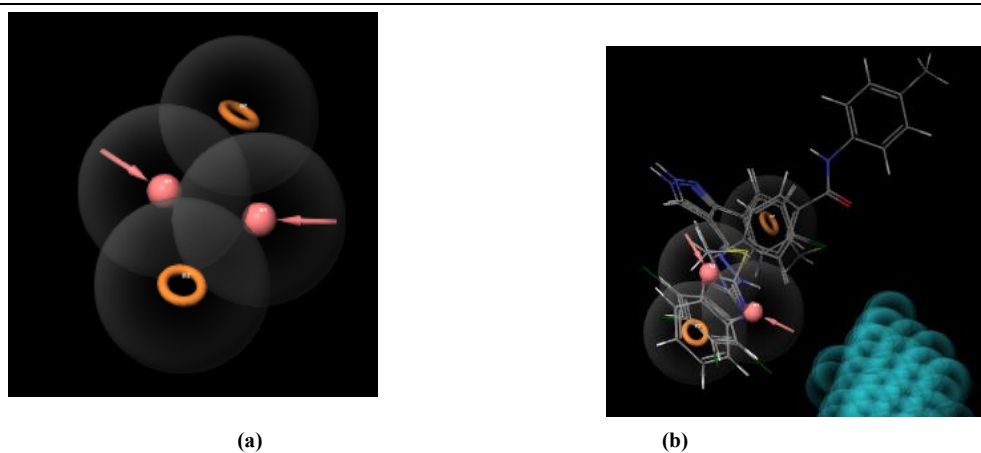


Figure 3.1.4: (a) A four point generated pharmacophore model (AARR_1) by PHASE module (b) Overlapping of the active ligands on pharmacophore model AARR_1

3.1.3 Statistical validation of Atom based 3D-QSAR model

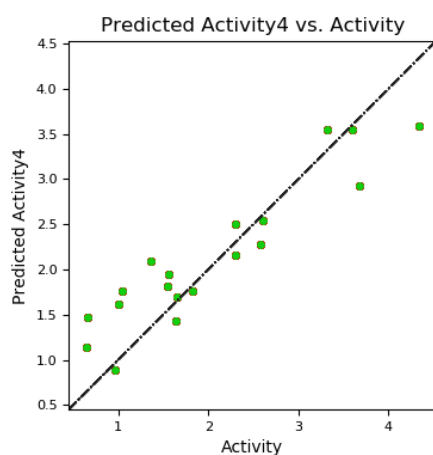
As the 3D-QSAR model was generated, it was validated for their reliability, robustness and stability. For the regression analysis the leave-one-out cross internal validation method was used by keeping the partial least square factor (PLS) 4. The internal validation report showed that the statistical parameters such as correlation coefficient for the training set ($Q^2 = 0.8129$), regression coefficient ($R^2 = 0.9440$), Scramble Fischer test ($F = 176.9$), a significance level of variance ratio ($P = 1.09e-25$), Standard deviation ($SD = 0.2339$), root mean square error ($RMSE = 0.46$) were found to be of good values for the generation of 3D-QSAR model (Table 3.1.3 and Table 3.1.4). Graphically, the scattered plots were shown for the test and training set depicting the values of the generated QSAR model (Figure 3.1.5).

Table 3.1.3: PLS parameters for the Atom based 3D-QSAR model.

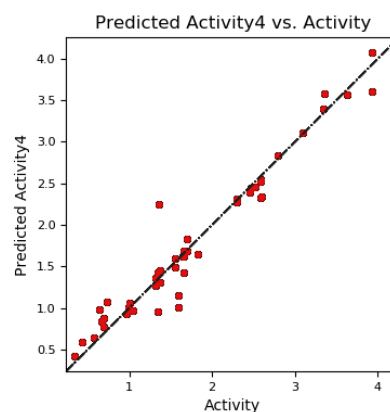
PLS Factor	SD	R2	F	P	Stability	Q2	RMSE	Pearson-R
1.	0.5642	0.6506	83.8	7.69e-12	0.863	0.7361	0.54	0.8641
2.	0.3941	0.8333	110.0	7.64e-18	0.67	0.8141	0.45	0.9215
3.	0.2712	0.9229	171.5	6.12e-24	0.461	0.8007	0.47	0.9274
4.	0.2339	0.9440	176.9	1.09e-25	0.453	0.8129	0.46	0.9281

Table 3.1.4: Statistical data of Atom based 3D-QSAR.

PLS Factors	HBD	Hydrophobic/ non-polar	Negative ionic	Positive ionic	e-withdrawing
1	0.040187	0.637762	0.025432	0.035507	0.218226
2	0.039857	0.624798	0.030728	0.035156	0.231427
3	0.042161	0.629142	0.028565	0.028649	0.237696
4	0.042973	0.635465	0.028433	0.026602	0.234998



(a)



(b)

Figure 3.1.5: Graphical representation of an observed activity (X-axis) v/s predicted activity (Y-axis) of (a) test set and (b) training set compounds of the hypothesis AARR_1. The best fit line for test set is $y = 0.68x + 0.76$ ($R^2 = 0.86$).

3.1.4 Computation of contour maps of Atom based 3D-QSAR model

3D-QSAR is a comprehensive method that uses a variety of statistical techniques to correlate the ligands' 3D features in order to predict their physiological and biological activities. Predicting biological activities is made necessary by the existence of several functional groups and moieties. Contour map depiction illustrates how the functional groups or moieties contribute to the compound's biological activity.

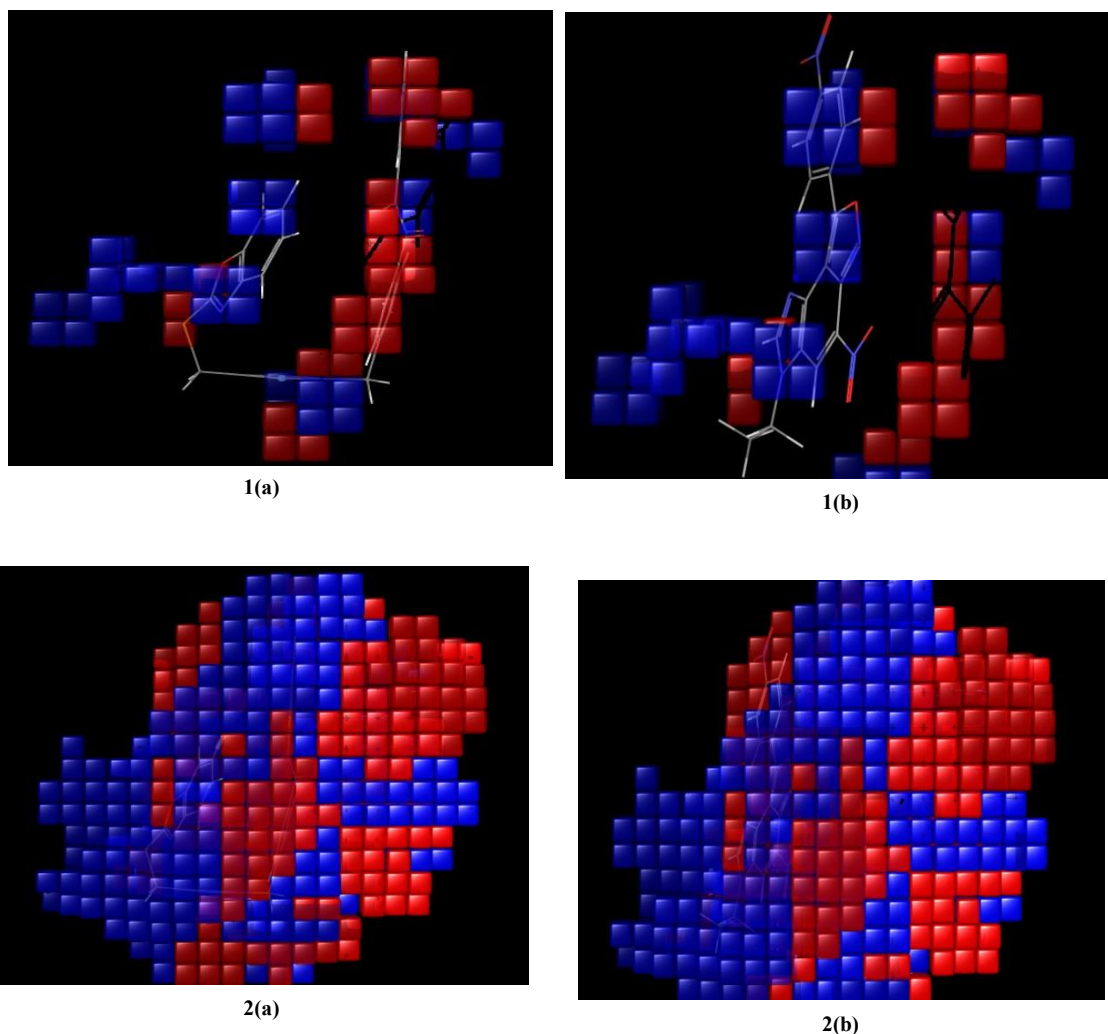
The maps' red areas represent the unfavorable interactions, while the blue areas highlight the advantageous characteristics that promoted interactions between enzymes and ligands. The hydrogen bond donor's atom-based 3D-QSAR contour map in Figure 3.1.6 (a) makes it easier to compare and see which groups or moieties are the most and least potent.

While the blue cubes surrounding the oxazole ring, phenyl ring, and C=O bond of the least active compound PC6 showed an increase in activity (Figure 3.1.6 (1b)), the red region around the phenyl ring indicates that a substitution is required to increase the activity, and the blue region around the oxazole ring of the most active compound PC7 (Figure 3.1.6 (1a)) indicates that a hydrogen bond donor is favorable for activity.

Furthermore, the hydrophobic map, as depicted in Figure 3.1.6 (2a), indicates that the large blue cubes covering the entire benzoxazole ring and the C-S group of the most active compound, PC7, are essential for the antimicrobial activity. However, the red region surrounding the phenyl ring suggests that some changes should be made to enhance the biological activity, in contrast to the red regions of the least active compound, PC6, which cover the NO₂ of the phenyl ring and NO₂ attached to the benzoxazole ring, which demonstrate the compound's decreased activity (Figure 3.1.6 (2b)).

Additionally, the e-withdrawing contour map of the most active compound, PC7 (Figure 3.1.6 (3a)), demonstrates that the blue region on the C-O-C bond of the oxazole ring, NH, and C=O attached to the alkyl chain shows a significant increase in activity, while the presence of red regions on the phenyl ring attached to the alkyl chain, benzene ring attached to the oxazole ring, and C-P bond shows a decline in activity due to the presence of electron-withdrawing group. Meanwhile, the presence of red cubes covering the entire compound, with the exception of the C=N group of five members, indicates a decline in the biological activity of the least active compound, PC6 (Figure 3.1.6 (3b)).

By the contour map visualization, the functional groups and its relation to the biological activity had been clarified.



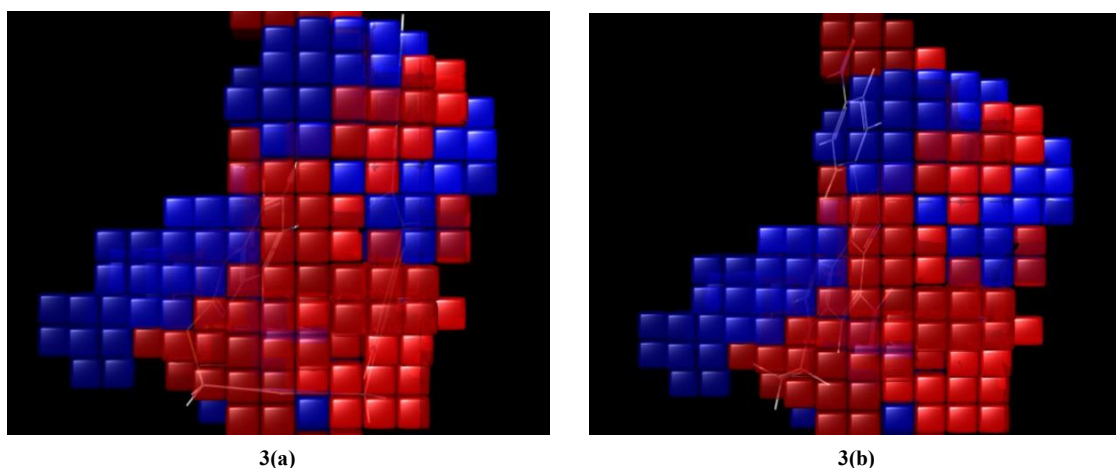


Figure 3.1.6: Visualization of Atom based 3D-QSAR model of most active compound

PC7 - 1(a) Hydrogen bond donor 2(a) Hydrophobic 3(a) Electron withdrawing and least active compound PC6 - 1(b) Hydrogen bond donor 2(b) Hydrophobic 3(b) Electron withdrawing Blue coloured cubes shows increase in activity and red coloured cubes shows decrease in activity.

3.1.5 ADME and toxicity profile prediction

The ADMET profiling of the top ten selected drug candidates was conducted using the QikProp module and the ProTox II online tool. All evaluated parameters were within the acceptable limits and complied with Lipinski's Rule of Five, which is essential for assessing drug-likeness. Compounds exhibiting optimal intestinal absorption and membrane permeability typically possess fewer than five hydrogen bond donors, fewer than ten hydrogen bond acceptors, a molecular weight under 500 Daltons, and a LogP value not exceeding 5. Key pharmacokinetic parameters, including the partition coefficient (LogP o/w ranging from -0.247 to 5.693), blood-brain barrier permeability (LogBB between 0.201 to -0.080), human serum albumin binding affinity (LogKhsa between -0.483 and 0.708), and skin permeability (P_{caco} values ranging from 1.196 to 5638.654), were analyzed to facilitate the identification of the most promising lead compounds (Table 3.1.5).

Insilco toxicity studies were conducted for predicting the toxicity and adverse effects of the selected top 10 drug hits by utilizing the ProTox II server which evaluated the results for hepatotoxicity, mutagenicity, carcinogenicity, immunotoxicity and cytotoxicity. The estimated results were taken into consideration by the predicted toxicity class level (I, II, III, IV, V and VI) and predicted median lethal dose (LD₅₀) in mg/kg weight. Based on the outcome data, compounds CID 174331251, CID 163955800, CID 175567519, CID 166872478, and CID 163583501 were classified under toxicity class IV, indicating a low level of acute toxicity. Among them, CID 163955800 and CID 163583501 exhibited an LD₅₀ value of 1600 mg/kg, reflecting a comparatively safer toxicity profile. Additionally, all organ toxicity parameters for these compounds were found to be inactive, further supporting their safety. These favorable findings highlight their strong potential for further exploration and development in future studies (Table 3.1.6).

Table 3.1.5: Top 10 drug hits ADME predictions by QikProp.

Entry	#Stars	Log p o/w	P caco	Log BB	#Metab	Log khsa	% human oral absorption	Rule of five
174377141	0	1.366	74.317	-1.950	5	-0.483	68.432	0
172743839	1	4.285	23.778	-1.055	4	0.045	76.665	0
162579096	1	5.693	284.519	-0.419	6	0.695	91.247	1
174331251	1	2.453	40.184	-1.6914	6	0.011	70.019	0
163955800	0	4.663	2502.390	-0.318	3	0.708	100	0
175567519	0	4.214	5121.852	-0.080	3	0.398	100	0
166872478	0	3.668	97.958	-1.351	4	0.027	84.055	0
163583501	0	4.094	5638.654	0.201	4	0.431	100	0
165521246	0	3.124	171.430	-0.993	5	-0.222	85.224	0
165349091	0	-0.247	1.196	-2.124	2	-1.120	26.982	0
Acceptable ranges		-2 -6.5	<25 poor; >500 good	-3- 1.2	1-8	-1.5-1.5	Max 100	Max 4

Table 3.1.6: Toxicity parameters of the top 10 drug hits by ProTox II tool.

Compounds	Classification					
	Organ toxicity	Toxicity end points				
	Hepatotoxicity	Carcinogenicity	Immunotoxicity	Mutagenicity	Cytotoxicity	Class
CID 174377141	Inactive	Inactive	Inactive	Inactive	Inactive	IV
CID 172743839	Active	Inactive	Inactive	Inactive	Inactive	IV

CID 162579096	Active	Active	Inactive	Inactive	Inactive	IV
CID 174331251	Inactive	Inactive	Inactive	Inactive	Inactive	IV
CID 163955800	Inactive	Inactive	Inactive	Inactive	Inactive	IV
CID 175567519	Inactive	Inactive	Inactive	Inactive	Inactive	IV
CID 166872478	Inactive	Inactive	Inactive	Inactive	Inactive	IV
CID 163583501	Inactive	Inactive	Inactive	Inactive	Inactive	IV
CID 165521246	Inactive	Inactive	Inactive	Active	Inactive	IV
CID 165349091	Inactive	Inactive	Inactive	Inactive	Inactive	IV

4.0 Summary

The present research work describes the antimicrobial activity of benzoxazole derivatives against the targeted protein dihydrofolate reductase by the Ligand-based drug design *in silico* approaches.

Ligand-based study was performed on 63 benzoxazole derivatives. Through Molecular docking studies compound PC7 emerges as the best docked compound with docking score (-8.572 kcal/mol). A ligand-based pharmacophore model was generated with AARR_1 as best hypothesis showed that two hydrogen bond acceptors and two aromatic ring feature are good for the activity. The Atom based 3D-QSAR model was built by utilizing the best generated hypotheses AAHR_1 and the internal validation showed that statistical parameters such as ($Q^2 = 0.8129$), ($R^2 = 0.9440$), ($SD = 0.2339$), and ($RMSE = 0.46$) were found to be good values for the built model. The best docked compound was performed for drug similarity in the PubChem database and molecular docking was carried out. The resulted top 10 hits were preceded to ADME/T predictions. From the resulting data it clarified that CID 163955800 and CID 163583501 have more potential as antimicrobial agents.

REFERENCES:-

- Capozzi C, Maurici M, Panà A. Antimicrobico resistenza: è crisi globale, "un lento tsunami" [Antimicrobial resistance: it is a global crisis, "a slow tsunami"]. *Ig Sanita Pubbl.* 2019 Nov-Dec;75(6):429-450. Italian. PMID: 32242168.
- Abushaheen MA, Fatani AJ, Alosaimi M, Mansy W, George M, Acharya S, Rathod S, Divakar DD, Jhugroo C, Vellappally S, Khan AA (2020) Antimicrobial resistance, mechanisms and its clinical significance. *Dis Mon* 66(6):100971.
- Lin S-K. Pharmacophore Perception, Development and Use in Drug Design. Edited by Osman F. Güner. *Molecules.* 2000;5:987-9.
- Kuntz ID, Blaney JM, Oatley SJ, Langridge R, Ferrin TE. A geometric approach to macromolecule-ligand interactions. *Journal of Molecular Biology.* 1982;161(2):269-88.
- Muddala, R., Waltermire, R. E., Suvarna, S., Xing, W., Han, Y., Fyans, J. K., & Hajduk, P. J. (2020). Structure-based design of dihydrophthalazine inhibitors targeting *Staphylococcus aureus* dihydrofolate reductase. *European Journal of Medicinal Chemistry*, 199, 112390.
- Strekowski L, Van Aken K. Three Heterocyclic Rings Fused (6: 5: 6). 2009.
- Vitaku E, Smith DT, Njardarson JTJ. Analysis of the structural diversity, substitution patterns, and frequency of nitrogen heterocycles among US FDA approved pharmaceuticals: miniperspective. 2014;57(24):10257-74.
- Ji Ram V, Sethi A, Nath M, Pratap RJOE. The Chemistry of Heterocycles. 2019:393-425.
- Kuntz ID, Blaney JM, Oatley SJ, Langridge R, Ferrin TE. A geometric approach to macromolecule-ligand interactions. *Journal of Molecular Biology.* 1982;161(2):269-88.
- Roy K, Kar S, Das RN. Chapter 9 - Newer QSAR Techniques. In: Roy K, Kar S, Das RN, editors. *Understanding the Basics of QSAR for Applications in Pharmaceutical Sciences and Risk Assessment.* Boston: Academic Press; 2015. p. 319-56.
- Padalkar VS, Borse BN, Gupta VD, Phatangare KR, Patil VS, Sekar N. Synthesis and Antimicrobial Activities of Novel 2-[substituted-1H-pyrazol-4-yl] Benzothiazoles, Benzoxazoles, and Benzimidazoles. 2016;53(5):1347-55.
- Ersan RH, Alagoz MA, Dogen A, Duran N, Burmaoglu S, Algul O. Bisbenzoxazole Derivatives: Design, Synthesis, in Vitro Antimicrobial, Antiproliferative Activity, and Molecular Docking Studies. *Polycyclic Aromatic Compounds.* 2022;42(6):3103-23.
- Tyagi R, Singh A, Chaudhary KK, Yadav MK. Chapter 17 - Pharmacophore modeling and its applications. In: Singh DB, Pathak RK, editors. *Bioinformatics: Academic Press;* 2022. p. 269-89.
- Roy K, Kar S, Das RN. Chapter 9 - Newer QSAR Techniques. In: Roy K, Kar S, Das RN, editors. *Understanding the Basics of QSAR for Applications in Pharmaceutical Sciences and Risk Assessment.* Boston: Academic Press; 2015. p. 319-56.
- Lengauer T, Rarey M. Computational methods for biomolecular docking. *Current Opinion in Structural Biology.* 1996;6(3):402-6.
- Zomorodian K, Khabnadideh S, Sakhteman A, Bi B, Mirjalili F, Ranjbar M, et al. SYNTHESIS AND ANTIFUNGAL ACTIVITY OF BENZOXAZOLE DERIVATIVES WITH THEIR SAR ANALYSIS BY SAS-MAP. 2020.
- Kumar M, Ramasamy K, Mani V, Mishra RK, Majeed ABA, De Clercq E, et al. Synthesis, antimicrobial, anticancer, antiviral evaluation and QSAR studies of 4-(1-aryl-2-oxo-1, 2-dihydro-indol-3-ylideneamino)-N-substituted benzene sulfonamides. *Arabian Journal of Chemistry.* 2014;7(4):396-408.
- J. Osipiuk JH, R. Jedrzejczak, E. Rubin, K. Guinn, D. Ioerger, T. Baker, J. Sacchettini, A. Joachimiak. Thymidylate synthase from *Staphylococcus aureus*. 2012.
- R.A. Friesner JLB, R.B. Murphy, T.A. Halgren, J.J. Klicic, D.T. Mainz, M.P. Repasky, E. H. Knoll, M. Shelley, J.K. Perry, and D.E. Shaw, . Glide: A new approach for rapid, accurate docking and scoring. Method and assessment of docking accuracy,. *J Med Chem.* 2004;47: 1739–49.
2022. LigPrep, Schrödinger, LLC, New York, NY. 2022.

17. Ertan-Bolelli T, Yildiz İ, Ozgen-Ozgacar S. Synthesis, molecular docking and antimicrobial evaluation of novel benzoxazole derivatives. *Medicinal Chemistry Research*. 2016;25(4):553-67.
18. Gupta S, Baweja GS, Gupta G, Asati V. Identification of potential N-substituted 5-benzylidenethiazolidine-2,4-dione derivatives as α -amylase inhibitors: Computational cum synthetic studies. 2023;1287:135596.
19. Manal M, Manish K, Sanal D, Selvaraj A, Devadasan V, Chandrasekar MJN. Novel HDAC8 inhibitors: A multi-computational approach. *SAR and QSAR in Environmental Research*. 2017;28(9):707-33.
20. Dixon SL, Smondyrev AM, Rao SN. PHASE: A Novel Approach to Pharmacophore Modeling and 3D Database Searching. 2006;67(5):370-2.
21. Golbraikh A, Tropsha A. Predictive QSAR modeling based on diversity sampling of experimental datasets for the training and test set selection. *Molecular Diversity*. 2000;5(4):231-43.
22. Mali S, Chaudhari H. Molecular modelling studies on adamantane-based Ebola virus GP-1 inhibitors using docking, pharmacophore and 3D-QSAR. *SAR and QSAR in Environmental Research*. 2019;30(3):161-80.
23. Sanapalli BKR, Yele V, Baldaniya L, Karri VVSR. Identification of novel protein kinase C- β II inhibitors: virtual screening, molecular docking and molecular dynamics simulation studies. *Journal of Molecular Modeling*. 2022;28(5):117.
24. Opo FADM, Rahman MM, Ahammad F, Ahmed I, Bhuiyan MA, Asiri AM. Structure based pharmacophore modeling, virtual screening, molecular docking and ADMET approaches for identification of natural anti-cancer agents targeting XIAP protein. *Scientific reports*. 2021;11(1):4049.
25. Gupta S, Baweja GS, Singh S, Irani M, Singh R, Asati VJEJoMC. Integrated fragment-based drug design and virtual screening techniques for exploring the antidiabetic potential of thiazolidine-2, 4-diones: Design, synthesis and in vivo studies. 2023;261:115826.